

# Medical Imaging

---

Prof. Dr. Tobias Knopp

6. Dezember 2022

Institut für Biomedizinische Bildgebung

# Magnetic Resonance Imaging

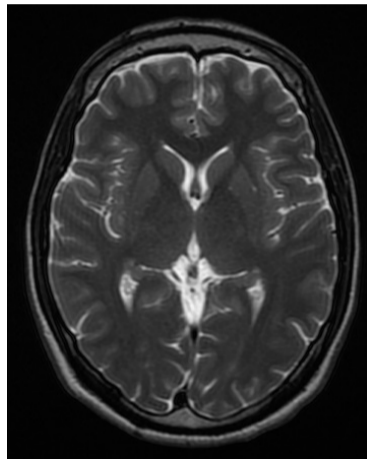
---

# Magnetic Resonance Imaging

- Tomographic imaging technique (usually 3D)
- Very good soft tissue contrast (CT just bones)
- No ionizing radiation
- Very flexible: allow generating different imaging contrast by modification of the imaging protocol
- In most cases one images the distribution of hydrogen in the human body

# Magnetic Resonance Imaging

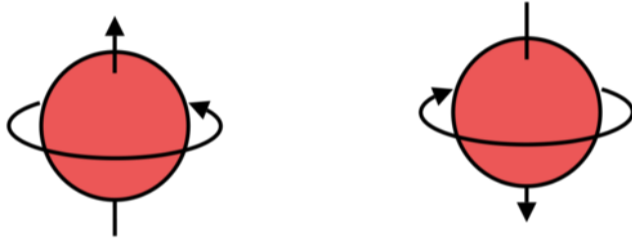
Left: Picture of a modern 3T MRI system. Right: Picture of a brain MRI scan.



- 1946: Discovery of the magnetic resonance principle by Bloch and Purcel (nobel price 1952)
- 1973: First tomographic image by Lauterbur (nobel price 2003)
- since 1984: MRI in clinical routine human body

## Basic Principle

Hydrogen atoms have a so-called *nuclear spin* leading to a magnetic dipole moment:

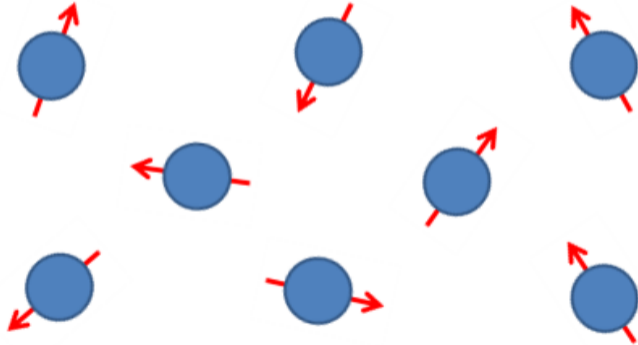


A classical picture would be a rotating atom, which establishes a magnetic moment  $m$ .

**Remark:** Precise description of MR physics requires quantum mechanics, which is beyond the scope of this lecture

## Basic Principle

Without an external magnetic field the magnetic moments have no preferred direction and follow a Boltzmann statistic (thermodynamic equilibrium):



# Magnetization

The magnetization is the (vectorial) sum of all individual magnetic moments relating to a small volume element  $\Delta V$ :

$$\mathbf{M} = \frac{1}{\Delta V} \sum_{j=0}^{N-1} \mathbf{m}_k \quad (1)$$

Due to the missing preferred direction of the nuclear spins the hydrogen atoms do not yield a measurable magnetization:

$$\Rightarrow \mathbf{M} = 0$$



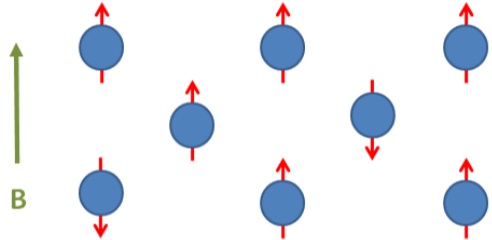
# $B_0$ Field

When applying a static (homogeneous) magnetic field

$$\mathbf{B}_0 = B_0 \begin{pmatrix} 0 \\ 0 \\ 1 \end{pmatrix}$$

the nuclear spins align with the magnetic field.

The magnetic moments either align in a parallel or in an anti-parallel way.



If both spin states would occur equally often, no macroscopic magnetization could be observed. However, fortunately, the state spin up occurs about  $10^{-6} \times B_0$  more often than the state spin down.

$\Rightarrow$  the stronger  $B_0$  the more spins are in the state spin up

Consequently, one observes a macroscopic magnetization that is aligned in  $z$  direction:

$$\mathbf{M} = M_0 \begin{pmatrix} 0 \\ 0 \\ 1 \end{pmatrix}$$

# Signal Encoding

---

A static magnetization is difficult to measure. In particular one cannot distinguish between the magnetization  $\mathbf{M}$  and the applied field  $\mathbf{B}_0$ . One thus needs a way to make  $\mathbf{M}$  and  $\mathbf{B}_0$  somehow different.

Ideas:

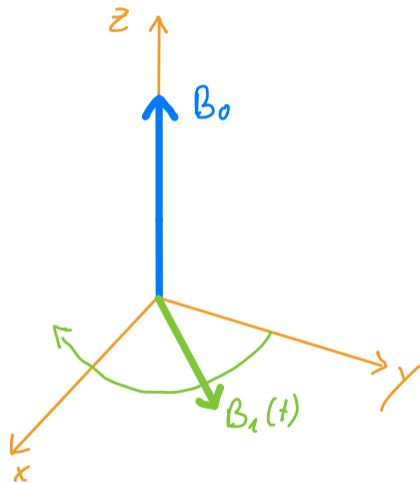
- Let  $\mathbf{M}$  point in a different direction than  $\mathbf{B}_0$
- Make  $\mathbf{M}$  time-dependent, since this allows use an inductive measurement

# Signal Encoding

To bring the magnetization into the  $xy$  plane, one applies a radio frequency field  $\mathbf{B}_1(t)$  that is orthogonal to  $\mathbf{B}_0$  and rotates in the  $xy$  plane.

$\mathbf{B}_1$  has an angular frequency  $\omega_E$  that matches the resonance frequency  $\omega_L$  of the nuclear spins.

$$\mathbf{B}_1 = B_1 \begin{pmatrix} \cos(\omega_E t) \\ \sin(\omega_E t) \\ 0 \end{pmatrix}$$



## Lamor Frequency and Gyromagnetic Ratio

The angular velocity  $\omega_L$  of the magnetization depends on the applied field strength  $B_0$  and the gyromagnetic ratio  $\gamma$ .

$$\omega_L = \gamma B_0$$

$\omega$  is named the *Lamor frequency*.

## Gyromagnetic Ratio

$\gamma$  depends on the considered matter:

Proton	$\gamma$ [MHz / T]
$^1\text{H}$	42.45
$^{13}\text{C}$	10.71
$^{19}\text{F}$	40.08
$^{15}\text{N}$	11.27
$^{31}\text{P}$	17.25

In MRI usually only the hydrogen atom is considered since the human consists of 65% water ( $\text{H}_2\text{O}$ ).

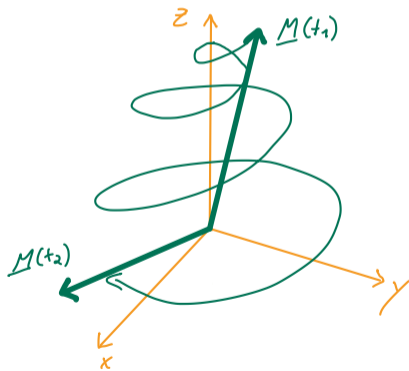
## Progression of Magnetization

Due to the  $90^\circ$  excitation, the magnetization is elongated in a spiral movement into the  $xy$  plane. This happens despite  $B_1 \ll B_0$  since the frequency of the  $B_1$  field matches the resonance frequency of the spins.

Thus, a magnetization

$$\mathbf{M}(t) = M_0 \begin{pmatrix} \cos(\omega_E t) \\ \sin(\omega_E t) \\ 0 \end{pmatrix}$$

is established.





# Relaxation

The varying magnetization can be measured using electromagnetic coils (induction principle).

However, the induced signal is shadowed by the inductively coupling signal of the rotating  $B_1$  field.

⇒ Switch off  $B_1$  field

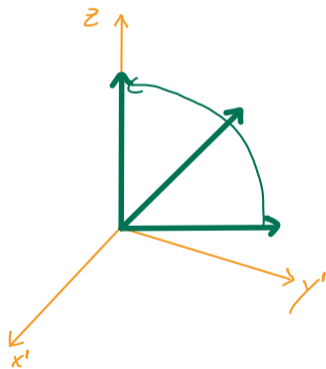
After switch off, the magnetization tries to align with the  $B_0$  field, which can be described by two different relaxation processes.

We consider on the following two slides a rotating coordinate system where the  $x'$  and  $y'$  coordinate rotate with the magnetization around the  $z$  axis and thus the magnetization would point would be static within the  $xy$  plane if no relaxation would occur.

# Longitudinal Relaxation

Increase of the z component of the magnetization

$$M_z = M_0(1 - e^{-\frac{t}{T_1}})$$

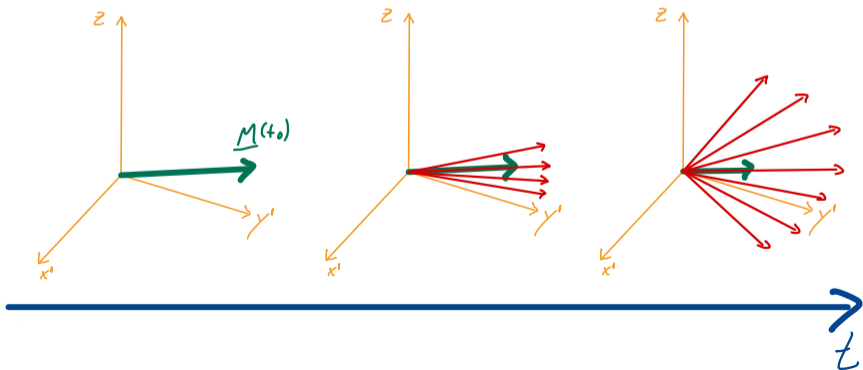


# Transversal Relaxation

Dephasing of the magnetic moments of the spins

$$M_{xy} = M_0 e^{-\frac{t}{T_2}}$$

⇒ After switching of the  $B_1$  field one can measure for a certain amount of time a magnetization signal in a receive coil.



## Magnetization after Excitation

Taking into account both relaxation processes, the magnetization after switching of the  $B_1$  field is given by

$$\mathbf{M}(t) = M_0 \begin{pmatrix} \cos(\omega_E t) e^{-t(\frac{1}{T_1} + \frac{1}{T_2})} \\ \sin(\omega_E t) e^{-t(\frac{1}{T_1} + \frac{1}{T_2})} \\ 1 - e^{-\frac{t}{T_1}} \end{pmatrix}$$

## Remarks

- At this point do not distinguish between the relaxation times  $T_2^*$  and  $T_2$  to keep the explanation simple. But note that what we described on the previous slide is actually called  $T_2^*$  ( $\frac{1}{T_2^*} = \frac{1}{T_2} + \frac{1}{T_{inhom}}$  see [https://en.wikipedia.org/wiki/Relaxation\\_\(NMR\)](https://en.wikipedia.org/wiki/Relaxation_(NMR)) for details).
- $T_2$  times are much faster than  $T_1$ . More precisely  $T_2^* \leq T_2 \leq T_1$ .
- $T_1$  and  $T_2$  are tissue dependent and give an additional contrast mechanism.

tissue	$T_1$ [ms]	$T_2$ [ms]
muscle	480	30
fat	190	60
gray brain matter	400	90
white brain matter	350	80

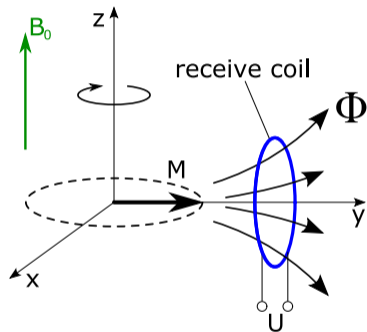
# Measurement of Magnetization

Induction law

$$u(t) = -\mu_0 \frac{d}{dt} \int_{\mathbb{R}^3} \mathbf{p}(\mathbf{r})^T \mathbf{M}(\mathbf{r}, t) d^3 r$$

where

- $u(t)$  is the voltage induced in the receive coil
- $\mathbf{p}(\mathbf{r})$  is the receive coil sensitivity
- $\mathbf{p}(\mathbf{r}) := \frac{\mathbf{B}(\mathbf{r})}{I}$ , magnetic field at unit current (1A)

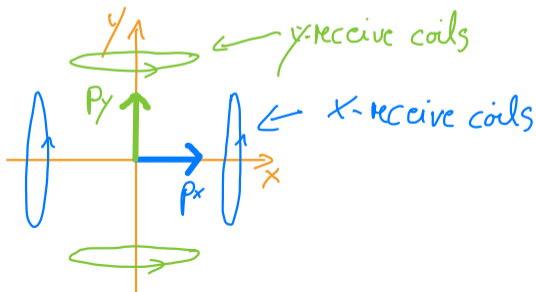


## Measurement of Magnetization

Since  $\mathbf{M}(t)$  rotates in the  $xy$  plane one uses two orthogonal receive coils with sensitivities

$$\mathbf{p}_x = \begin{pmatrix} p \\ 0 \\ 0 \end{pmatrix} \quad \text{and} \quad \mathbf{p}_y = \begin{pmatrix} 0 \\ p \\ 0 \end{pmatrix}$$

For instance two Helmholtz coil pairs can be used:



## Measurement of Magnetization

In turn the induced signals are given by

$$u_x(t) = -\mu_0 \rho \int_{\mathbb{R}^3} \frac{d}{dt} M_x(\mathbf{r}, t) d^3 r$$

$$u_y(t) = -\mu_0 \rho \int_{\mathbb{R}^3} \frac{d}{dt} M_y(\mathbf{r}, t) d^3 r$$



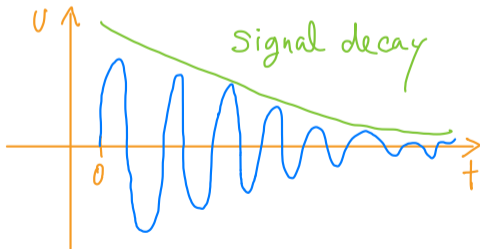
## Measurement of Magnetization

If we consider for a moment only the signal from a single voxel in the center we obtain:

$$u_x(t) = -\mu_0 \rho \frac{d}{dt} \cos(\omega_E t) e^{-t(\frac{1}{T_1} + \frac{1}{T_2})}$$

$$u_y(t) = -\mu_0 \rho \frac{d}{dt} \sin(\omega_E t) e^{-t(\frac{1}{T_1} + \frac{1}{T_2})}$$

Thus, due to dephasing the signal decays exponentially. This is also called Free Induction Decay (FID).



# Assumptions

We will in the following neglect relaxation effects. In practice this means that one has to measure fast enough that the dephasing did not progress too far. In practice one will apply several excitations.

In turn our model for the magnetization will be

$$\mathbf{M}(\mathbf{r}, t) = M_0(\mathbf{r}) \begin{pmatrix} \cos(\omega_E t) \\ \sin(\omega_E t) \\ 0 \end{pmatrix}$$

## Signal Equation

Consequently the signal equations are given by

$$u_x(t) = -\mu_0 \rho \int_{\mathbb{R}^3} \frac{d}{dt} M_0(\mathbf{r}) \cos(\omega_E t) d^3 r$$
$$u_y(t) = -\mu_0 \rho \int_{\mathbb{R}^3} \frac{d}{dt} M_0(\mathbf{r}) \sin(\omega_E t) d^3 r$$

yielding

$$u_x(t) = \mu_0 \rho \omega_E \int_{\mathbb{R}^3} M_0(\mathbf{r}) \sin(\omega_E t) d^3 r$$
$$u_y(t) = -\mu_0 \rho \omega_E \int_{\mathbb{R}^3} M_0(\mathbf{r}) \cos(\omega_E t) d^3 r$$

One can combine both equations by mapping the voltages on the complex plane:

$$\begin{aligned}u_{xy}(t) &= -u_y(t) + iu_x(t) \\ &= \mu_0 p \omega_E \int_{\mathbb{R}^3} M_0(\mathbf{r}) (\cos(t\omega_E) + i \sin(t\omega_E)) d^3 r \\ &= \mu_0 p \omega_E \int_{\mathbb{R}^3} M_0(\mathbf{r}) e^{it\omega_E} d^3 r\end{aligned}$$

# Spatial Encoding

---

Until now all spins in space behave the same

⇒ No image can be obtained.

## **Slice Selection**

Idea: not all spins in space are excited but only those within a certain slice. To this end, a *gradient* is applied *during excitation*:

$$B_z(z) = B_0 + zG_z$$

The field thus increases linearly in  $z$  direction.

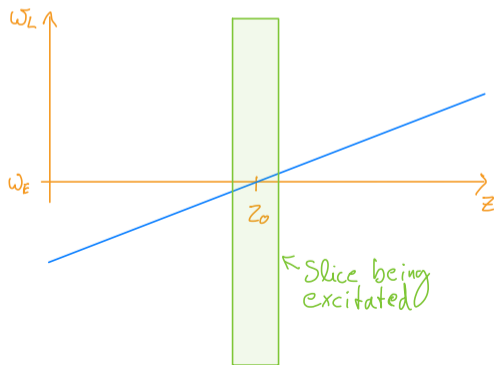
# Spatial Encoding

Lamor frequency

$$\omega_L(z) = \gamma B_z(z) = \gamma(B_0 + zG_z)$$

is now slice dependent.

⇒ chose  $\omega_E$  of the  $B_1$  excitation such that  $\omega_L(z_0) = \omega_E$  if the slice  $z_0$  should be excited.



The signal equation due to slice selection becomes

$$u_{xy}(t) = \mu_0 \rho \omega_E \int_{\mathbb{R}^2} M_0(x, y) e^{it\omega_E} dx dy$$



# Spatial Encoding

By slice selection all spins within a certain slice are excited.

But within the slice still all spins behave the same

⇒ Next step: spatial encoding within plane

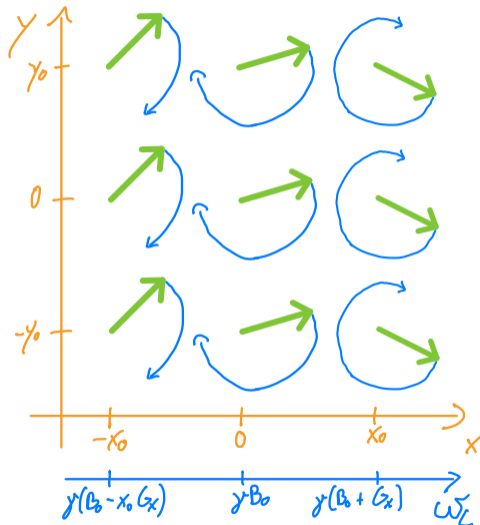
# Frequency Encoding

- Change angular frequency of magnetization *during data acquisition*.
- This is done by applying a gradient field that changes the z component of the magnetic field linearly in the x direction:

$$B_z(x) = B_0 + xG_x$$

- The Larmor frequency is thus given by

$$\omega_L(x) = \gamma B_z(x) = \gamma(B_0 + xG_x) = \omega_0 + \gamma x G_x$$



## Frequency Encoding

Due to frequency encoding, the frequency of the magnetization gets spatially dependent:

$$u_{xy}(t) = \mu_0 \rho \omega_E \int_{\mathbb{R}^2} M_0(x, y) e^{it(\omega_0 + \gamma x G_x)} dx dy$$

We now can pull out the carrier frequency  $e^{it\omega_0}$  yielding

$$u_{xy}(t) = \mu_0 \rho \omega_E e^{it\omega_0} \int_{\mathbb{R}^2} M_0(x, y) e^{it\gamma x G_x} dx dy$$

Thus, by dividing the induced signal by  $\mu_0 \rho \omega_E e^{it\omega_0}$  one obtains

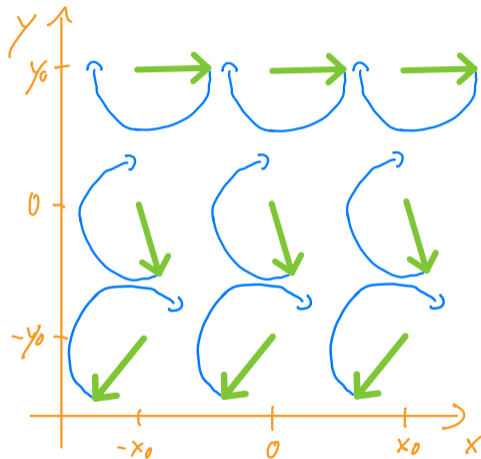
$$\tilde{u}_{xy}(t) = \frac{u_{xy}(t)}{\mu_0 \rho \omega_E e^{it\omega_0}} = \int_{\mathbb{R}^2} M_0(x, y) e^{it\gamma x G_x} dx dy$$

This is a Fourier integral along the  $x$  direction.

Missing: Spatial encoding in  $y$  direction.

# Phase Encoding

- **Idea:** Apply gradient *before* data acquisition.
- ⇒ accelerates the precession (positively and negatively) of the magnetization for a short time.
- ⇒ phase of magnetization is linearly varying in  $y$  direction.
- ⇒ spatial encoding achieved.



## Phase Encoding

Since the phase encoding was applied *before* data acquisition, the magnetization is rotating with  $e^{i(t\omega_E + \phi_y)}$  where  $\phi_y$  is the phase that depends on the duration and strength of the phase encoding gradient. We chose the time such that  $\phi_y = \gamma y G_y t$  such that the imaging equation *during* data acquisition becomes

$$\tilde{u}_{xy}(t) = \int_{\mathbb{R}^2} M_0(x, y) e^{i(t\gamma x G_x + \gamma y G_y t)} dx dy$$

If we define  $k_x = \frac{\gamma G_x t}{2\pi}$  and  $k_y = \frac{\gamma G_y t}{2\pi}$  we obtain a regular 2D Fourier integral

$$\tilde{u}_{xy}(k_x, k_y) = \int_{\mathbb{R}^2} M_0(x, y) e^{2\pi i(xk_x + yk_y)} dx dy$$

In order to fill the entire Fourier space (also named *k-space*) several excitations with different phase encodings have to be applied.

# Image Reconstruction

We have derived a special imaging equation for 2D sequences. More general, the MRI signal equation can be written as

$$s(\mathbf{k}) = \int_{\mathbb{R}^3} M_0(\mathbf{r}) e^{2\pi i \mathbf{k}^T \mathbf{r}} d^3 r$$

where  $\mathbf{r} = \begin{pmatrix} x \\ y \\ z \end{pmatrix}$  and  $\mathbf{k} = \begin{pmatrix} k_x \\ k_y \\ k_z \end{pmatrix}$

After applying the Fourier inversion theorem one obtains

$$M_0(\mathbf{r}) = \int_{\mathbb{R}^3} s(\mathbf{k}) e^{-2\pi i \mathbf{k}^T \mathbf{r}} d^3 k$$

## Remarks

- Image reconstruction thus can be done explicitly. In the discrete setting it corresponds to a matrix-vector operation that usually can be performed by the FFT in an  $\mathcal{O}(N \log N)$  fashion.
- Image reconstruction in MRI is thus **not** an ill-posed inverse problem.
- In practice one often applies subsampling in which case the inverse problem again gets ill-posed.
- When choosing the gradient trajectory  $\mathbf{k}(t)$  nonequidistantly, the FFT needs to be replaced by the NFFT, which is discussed in the next lecture.
- Inhomogeneous coils and relaxation times lead to more complicated signal models when being taken into account.



# Pulse Sequences

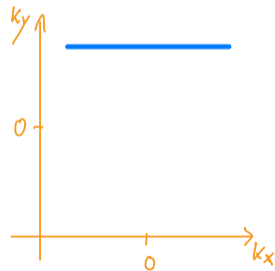
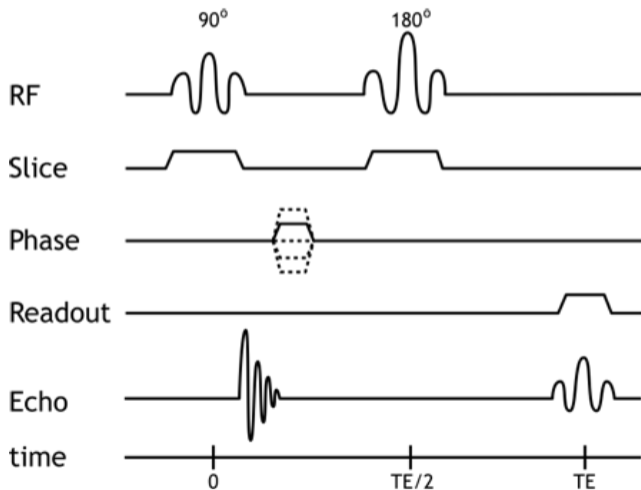
---

The applied dynamic magnetic fields during an MR acquisition can be expressed using a *pulse sequence diagram*.

In this lecture only a quick overview about basic pulse sequences is given.

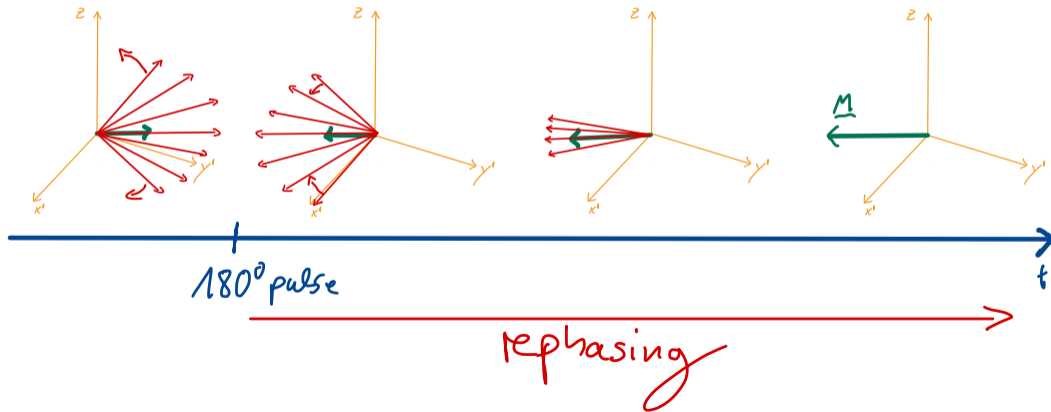
# Spin Echo Sequence

Basic *spin echo sequence*. The  $180^\circ$  pulses are necessary to rephase the spins.



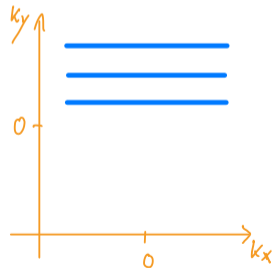
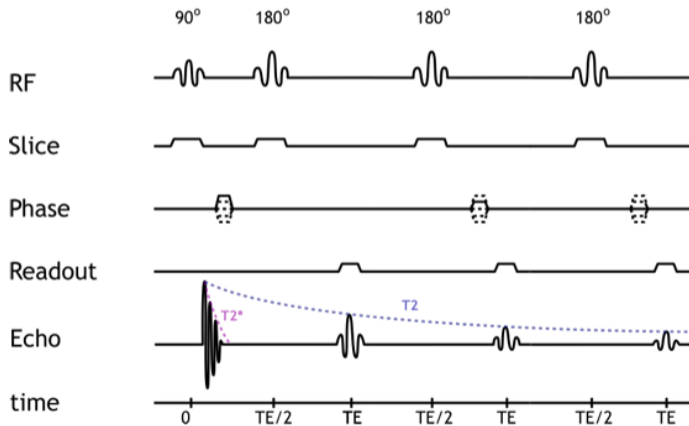
# 180° Pulse

The 180° degree pulse flips the drifting (macroscopic) magnetic moments (ensembles of similar phasing magnetic moments). Due to the flip, the moments align and a measurable magnetization is established again.



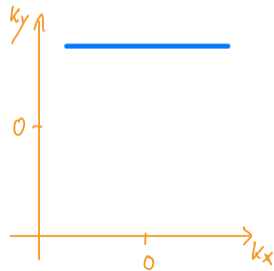
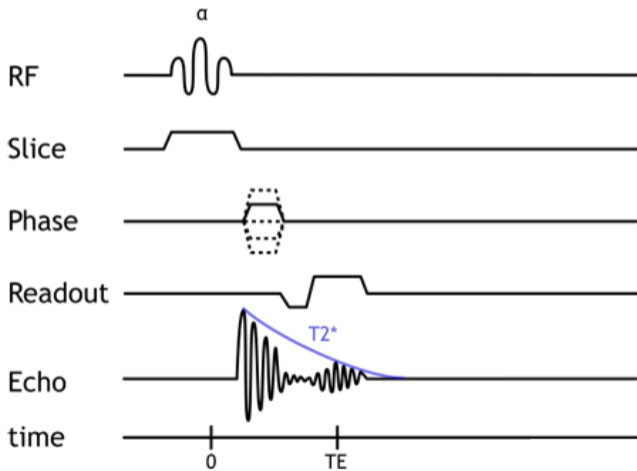
# Fast Spin Echo Sequence

Use multiple 180 degree pulses to speed up data acquisition.



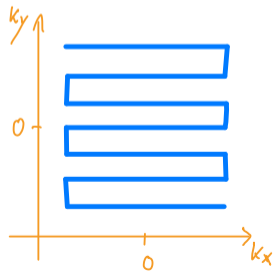
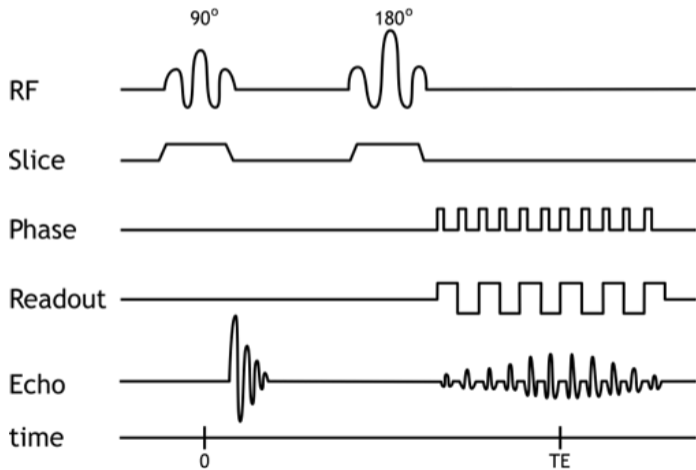
# Gradient Echo Sequence

Echos can also be generated by gradients (even faster).



# Echo Planar Imaging Sequence

One can also measure several phase encoding gradients within a single excitation.



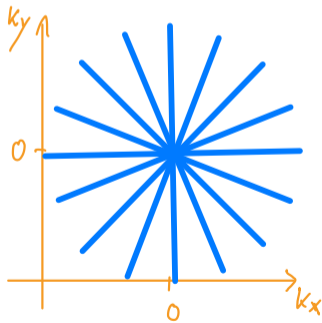
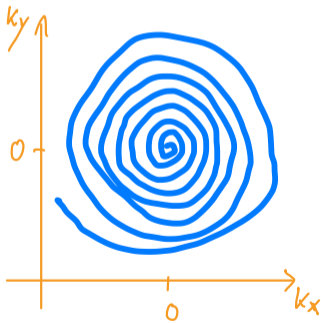
# Sampling Trajectories

---



## Nonequidistant Sampling Trajectories

Changing the gradients  $G_x$  and  $G_y$  both continuously during data acquisition allows for arbitrary  $k$ -space sampling. Beside Cartesian trajectories also non-equidistant trajectories can be applied. Spiral trajectories (left) allow for collecting more data within a single excitation. Radial trajectories (right) are robust against motion.

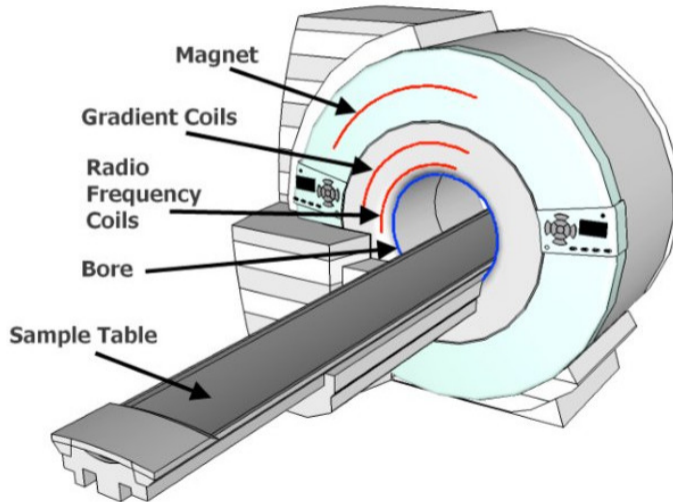


# System Overview

---

# System Overview

Schematic overview of a typical MRI scanner including the three field generators.



- MRI is a versatile imaging modality.
- It has long scan times due to sequential data collection.
- Basic image reconstruction is simple and just an FFT ( $\rightarrow$  not noise amplifying).
- Nonequidistant trajectories require the NFFT.
- Subsampling and field imperfection lead to more sophisticated image reconstruction methods.